Linear Parameter-Varying Spectral Decomposition

Bagge Carlson, Fredrik; Robertsson, Anders; Johansson, Rolf

Published in:
American Control Conference (ACC), 2017

DOI:
10.23919/ACC.2017.7962945

2017

Document Version:
Early version, also known as pre-print

Linear Parameter-Varying Spectral Decomposition

Fredrik Bagge Carlson* Anders Robertsson Rolf Johansson

***Abstract*— A linear parameter-varying (LPV) spectral decomposition method, based on least-squares estimation and kernel expansions, is developed. Statistical properties of the estimator are analyzed and verified in simulations. The method is linear in the parameters, applicable to both the analysis and modeling problems and is demonstrated on both simulated signals as well as measurements of the torque in an electrical motor.**

***Index Terms*— System Identification, Spectral Estimation, Spectral Decomposition, LPV-modeling**

I. Introduction

Standard spectral density estimations techniques such as the discrete Fourier transform (DFT) exhibit several well-known limitations. These methods are typically constructed for data sampled equidistantly in time or space. Whenever this fails to hold, typical approaches employ some interpolation technique in order to perform spectral estimation on equidistantly sampled data. Other possibilities include employing a method suitable for non-equidistant data, such as least-squares spectral analysis [1]. Fourier transform-based methods further suffer from spectral leakage due to the assumption that all sinusoidal basis functions are orthogonal over the data window [2]. Least-squares spectral estimation takes the correlation of the basis functions into account and further allows for estimation of arbitrary/known frequencies without modification [1].

In some applications, the spectral content is varying with an external variable, for instance, a controlled input. As motivating example, we consider the torque ripple induced by the rotation of an electrical motor. Spectral analysis of the torque signal is made difficult by equidistant, time-based sampling, which causes the spectrum to vary with the velocity of the motor, both due to the frequency of the ripple being directly proportional to the velocity, but also due to the properties of an electric DC-motor. A higher velocity both induces higher magnitude torque ripple, but also a higher filtering effect due to the inertia of the rotating parts. The effect of a sampling delay on the phase of the measured ripple is similarly proportional to the velocity.

*An open-source implementation of the method is available at `https://github.com/baggepinnen/LPVSpectral.jl`. The reported research was supported by the European Commission under the Framework Programme Horizon 2020 under grant agreement 644938 SARAFun.

Lund University, Dept Automatic Control, PO Box 118
SE22100 Lund Sweden
Fredrik.Bagge_Carlson@control.lth.se

Time-frequency analysis traditionally employ windowing techniques [3] in order to reduce spectral leakage [4], [5], mitigate effects of non-stationarity, reduce the influence of ill-posed autocorrelation estimates [5] and allow for time-varying spectral estimates [2]. The motivating example considers estimation of the spectral content of a signal which is periodic over the space of angular positions $\mathcal{X}$, with a spectral content varying with time solely due to the fact that the velocity is varying with time. Time does thus not hold any intrinsic meaning to the modification of the spectrum, and the traditional windowing in time is no longer essential.

This paper develops a spectral estimation technique using basis function expansions identified with the least-squares method, that allows the spectral properties (phase and amplitude) of the analyzed signal to vary with an external signal. Apart from a standard spectrum, functional relationships between the scheduling signal and the amplitude and phase of each frequency will be identified.

II. LPV Spectral Decomposition

A. Basis function expansions

In order to decompose the spectrum along an external dimension, we consider basis function expansions. Intuitively, a basis function expansion decomposes an intricate function or signal as a linear combination of simple basis functions. The Fourier transform can be given this interpretation, where an arbitrary signal is decomposed as a sum of complex-valued sinusoids, similarly, a stair function can be decomposed as a sum of step functions. With this intuition, we aim for a method which allow decomposition of the spectrum of a signal along an external dimension, in LPV terminology called the scheduling dimension, $\mathcal{V}$. If we consider a single sinusoid in the spectrum, the functional dependence decomposed by the basis function expansion will thus be the complex-valued coefficient k in $ke^{i\omega}$ as a function of the scheduling variable, v, which in the motivating example is the angular velocity of the motor. Using complex valued calculations, we simultaneously model the dependence of both amplitude and phase of a real frequency by considering the complex frequency.

Radial Basis Functions (RBFs) have been widely used in nonlinear modeling through RBF expansions or RBF networks [6]. The motivation for considering RBFs as opposed to other basis functions include their, in practice, local support, which often make the modeling more

intuitive and the result easier to interpret. This in contrast to basis functions with global support, such as sigmoid-type functions. Another motivation for the use of RBFs is the implicit assumption that the underlying functional dependence is smooth. The method proposed in this paper is not limited to the use of RBFs as basis functions, and extend without difficulty to other basis functions when motivated. A typical set of RBFs is shown in Fig. 1.

B. Least-squares identification of periodic signals

This paper deals with estimations of models which are linear in the parameters, and can thus be written on the form

$$y = \mathbf{A}k \tag{1}$$

where $\mathbf{A}$ denotes a regressor matrix and k denotes a vector of coefficients to be identified. Models on the form (1) are commonly identified with the well-known least-squares procedure [3]. For the model $y(n) = k_1 \sin(\omega n) + k_2 \cos(\omega n)$, this amounts to arranging the data according to

$$y = \begin{bmatrix} y(1) \\ \vdots \\ y(N) \end{bmatrix}, \quad \mathbf{A} = \begin{bmatrix} \sin(\omega 1) & \cos(\omega 1) \\ \vdots & \vdots \\ \sin(\omega N) & \cos(\omega N) \end{bmatrix} \in \mathbb{R}^{N\times 2}$$

$$k = \begin{bmatrix} k_1 & k_2 \end{bmatrix}^\mathsf{T}$$

and solving the optimization problem[1] of Eq. (2) with solution (3).

$$k^* = \arg\min_k \left\| \mathbf{A}k - y \right\|_2 \tag{2}$$

$$= (\mathbf{A}^\mathsf{T}\mathbf{A})^{-1}\mathbf{A}^\mathsf{T}y \tag{3}$$

This can be written in compact form by noting that $e^{i\omega} = \cos\omega + i\sin\omega$, which will be used extensively throughout the paper to simplify notation.[2]

We will now proceed to formalize a method for spectral decomposition using a perspective based on basis function expansions.

C. Model

We start by establishing some notation. Let k denote the Fourier series coefficients of interest. The kernel activation vector $\phi(v_n) : (v \in \mathcal{V}) \to \mathbb{R}^K$ maps the input to a set of basis function activations and is given by

$$\phi(v_n) = \begin{bmatrix} \kappa(v_n, \theta_1) & \cdots & \kappa(v_n, \theta_J) \end{bmatrix}^\mathsf{T} \in \mathbb{R}^J \tag{4}$$

$$\kappa(v, \theta_j) = \kappa_j(v) = \exp\left(-\frac{(v-\mu_j)^2}{2\sigma_j^2} \right) \tag{5}$$

where κ is a basis function parameterized by $\theta_j = (\mu_j, \sigma_j)$, $\mu \in \mathcal{V}$ is the center of the kernel and σ^2 is determining the width.

[1]This problem can easily be solved also for other norms or convex loss functions.

[2]Note that solving the complex LS problem using complex regressors $e^{i\omega}$ is not equivalent to solving the real LS problem using sin/cos regressors.

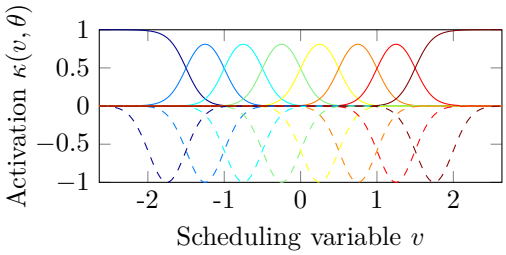

Fig. 1. Gaussian (dashed) and normalized Gaussian (solid) windows. Regular windows are shown mirrored in the x-axis for clarity.

Let y denote the signal to be decomposed and denote the location of the sampling of y_n by $x_n \in \mathcal{X}$. The space $\mathcal{X}$ is commonly time or space, in the motivating example of the electrical motor, $\mathcal{X}$ is the space of motor positions.[3] Let the intensities of a set of complex frequencies $i\omega \; \forall \; \omega \in \Omega$ be given by basis function expansions along $\mathcal{V}$, according to

$$\hat{y}_n = \sum_{\omega\in\Omega} \sum_{j=1}^{J} k_{\omega,j} \, \kappa_j(v_n) e^{-i\omega x_n} \tag{6}$$

$$= \sum_{\omega\in\Omega} k_\omega^\mathsf{T} \, \phi(v_n) e^{-i\omega x_n}, \quad k_\omega \in \mathbb{C}^J \tag{7}$$

The complex coefficients to be estimated, $k \in \mathbb{C}^{O\times J}$, $O = \text{card}(\Omega)$, constitute the Fourier series coefficients, with intensities split over $\mathcal{V}$. This formulation reduces to the standard Fourier style spectral relation (8) in the case $\phi(v) \equiv 1$

$$\hat{y} = \sum_{\omega\in\Omega} k_\omega \, e^{-i\omega x} = \Phi k \tag{8}$$

where $\Phi = [e^{-i\omega_1 x} \; ... \; e^{-i\omega_O x}]$. If the number J of basis functions equals the number of data points N, the model will exactly interpolate the signal, i.e., $\hat{y} = y$. If in addition to $J = N$, the basis function centers are placed at $\mu_j = v_j$, we obtain a Gaussian process regression interpretation where κ is the covariance function. Due to the numerical properties of the analytical solution of the least-squares problem, it is often beneficial to reduce the number of parameters significantly, so that $J \ll N$. If the chosen basis functions are suitable for the signal of interest, the error induced by this dimensionality reduction is small. In a particular case, the number of RBFs to include, J, and the bandwidth Σ is usually chosen based on evidence maximization or cross validation [6].

To facilitate estimation of the parameters in Eq. (6), we rewrite the model by stacking the regressor vectors in a regressor matrix A, see Sec. II-B, such that

$$\mathbf{A}_{n,:} = \text{vec}\left(\phi(v_n)\Phi^\mathsf{T}\right)^\mathsf{T} \in \mathbb{C}^{O\cdot J}, n = 1...N$$

We further define $\tilde{\mathbf{A}}$ by expanding the regressor matrix into its real and imaginary parts

$$\tilde{\mathbf{A}} = \begin{bmatrix} \Re\mathbf{A} & \Im\mathbf{A} \end{bmatrix} \in \mathbb{R}^{N\times 2OJ}$$

[3]We note at this stage that $x \in \mathcal{X}$ can be arbitrarily sampled and are not restricted to lie on an equidistant grid, as is the case for, e.g., Fourier transform-based methods.

such that routines for real-valued least-squares problems can be used. The complex coefficients are, after solving the real-valued problem (3), retrieved as $k = \Re k + i\Im k$ where

$$[\Re k^\intercal \quad \Im k^\intercal]^\intercal = \arg\min_{\tilde{k}} \left\| \tilde{\mathbf{A}}\tilde{k} - y \right\|_2$$

Since the purpose of the decomposition is spectral analysis, it is important to normalize the basis function activations such that the total activation over $\mathcal{V}$ for each data point is unity, to this end, the expressions (6) and (7) are modified to

$$\begin{aligned} \hat{y} &= \sum_{\omega\in\Omega}\sum_{j=1}^{J} k_{\omega,j}\,\bar{\kappa}_j(v)e^{-i\omega x} \\ &= \sum_{\omega\in\Omega} k_\omega^\intercal\,\bar{\phi}(v)e^{-i\omega x} \\ \bar{\kappa}_j(v) &= \frac{\kappa_j(v)}{\sum_j \kappa_j(v)}, \quad \bar{\phi}(v) = \frac{\phi(v)}{\sum \phi(v)} \end{aligned} \tag{9}$$

This ensures that the spectral content for a single frequency ω is a convex combination of contributions from each basis function in the scheduling dimension. Without this normalization, the power of the spectrum would be ill-defined and depend on an arbitrary scaling of the basis functions. The difference between a set of Gaussian functions and a set of normalized Gaussian functions is demonstrated in Fig. 1. The normalization performed in Eq. (9) can be viewed as the kernel function being made data adaptive by normalizing $\phi(v)$ to sum to one.

D. Amplitude and phase functions

In spectral analysis, two functions of the Fourier series coefficients are typically of interest, the amplitude and phase functions, which are easily obtained and are stated here without proof:

Proposition 1: Let a signal y be composed by the linear combination $y = k_1\cos(x) + k_2\sin(x)$, then y can be written on the form

$$y = A\cos(x - \varphi)$$

with

$$A = \sqrt{k_1^2 + k_2^2} \qquad \varphi = \arctan\left(\frac{k_2}{k_1}\right)$$

From this we obtain the following two functions for a single frequency ω

$$\begin{aligned} A(\omega) &= |k_\omega| = \sqrt{\Re k_\omega{}^2 + \Im k_\omega{}^2} \\ \varphi(\omega) &= \arg(k_\omega) = \arctan\left(\Im k_\omega / \Re k_\omega\right) \end{aligned}$$

In the proposed spectral decomposition method, these functions are further dependent on v, and are approximated by

$$A(\omega, v) = \left| \sum_{j=1}^{J} k_{\omega,j}\,\bar{\kappa}(v) \right| = \left| k_\omega^\intercal\,\bar{\phi}(v) \right| \tag{10}$$

$$\varphi(\omega, v) = \arg\left(\sum_{j=1}^{J} k_{\omega,j}\bar{\kappa}(v) \right) = \arg\left(k_\omega^\intercal\,\bar{\phi}(v) \right) \tag{11}$$

E. Covariance properties

We will now investigate and prove that Eq. (10) and Eq. (11) lead to asymptotically unbiased and consistent estimates of A and φ and will provide a strategy to obtain confidence intervals. We will initially consider a special case for which analysis is simple, whereafter we invoke the RBF universal approximation results of Park [7] to show that the estimators are well motivated for a general class of functions. We start by considering signals on the form Eq. (12), for which unbiased and consistent estimates of the parameters are readily available:

Proposition 2: Let a signal y be given by

$$\begin{aligned} y &= a(v)\cos(x) + b(v)\sin(x) + e \\ a(v) &= \alpha^\intercal\phi_v \\ b(v) &= \beta^\intercal\phi_v \\ e &\in \mathcal{N}(0, \sigma^2) \end{aligned} \tag{12}$$

with $\phi_v = \phi(v)$ and let $\hat{\alpha}$ and $\hat{\beta}$ denote unbiased estimates of α and β, then

$$\hat{A}(\hat{\alpha}, \hat{\beta}) = \sqrt{\left(\hat{\alpha}^\intercal\phi_v\right)^2 + \left(\hat{\beta}^\intercal\phi_v\right)^2} \tag{13}$$

is a biased estimate of A with

$$A < \mathbb{E}\left\{\hat{A}\right\} < \sqrt{A^2 + \phi_v^\intercal\Sigma_\alpha\phi_v + \phi_v^\intercal\Sigma_\beta\phi_v} \tag{14}$$

Proof: Since α, β and e appear linearly in Eq. (12), unbiased and consistent estimates $\hat{\alpha}$ and $\hat{\beta}$ are available from the least-squares procedure [3]. The expected value of $\hat{A}^2$ is given by

$$\begin{aligned} \mathbb{E}\left\{\hat{A}^2\right\} &= \mathbb{E}\left\{\left(\hat{\alpha}^\intercal\phi_v\right)^2 + \left(\hat{\beta}^\intercal\phi_v\right)^2\right\} \\ &= \mathbb{E}\left\{\left(\hat{\alpha}^\intercal\phi_v\right)^2\right\} + \mathbb{E}\left\{\left(\hat{\beta}^\intercal\phi_v\right)^2\right\} \end{aligned} \tag{15}$$

We further have

$$\begin{aligned} \mathbb{E}\left\{\left(\hat{\alpha}^\intercal\phi_v\right)^2\right\} &= \mathbb{E}\left\{\hat{\alpha}^\intercal\phi_v\right\}^2 + \mathbb{V}\left\{\hat{\alpha}^\intercal\phi_v\right\} \\ &= \left(\alpha^\intercal\phi_v\right)^2 + \phi_v^\intercal\Sigma_\alpha\phi_v \end{aligned} \tag{16}$$

where Σ_α and Σ_β are the covariance matrices of $\hat{\alpha}$ and $\hat{\beta}$ respectively. Calculations for β are analogous. From Eqs. (15) and (16) we deduce

$$\begin{aligned} \mathbb{E}\left\{\hat{A}^2\right\} &= \left(\alpha^\intercal\phi_v\right)^2 + \left(\beta^\intercal\phi_v\right)^2 + \phi_v^\intercal\Sigma_\alpha\phi_v + \phi_v^\intercal\Sigma_\beta\phi_v \\ &= A^2 + \phi_v^\intercal\Sigma_\alpha\phi_v + \phi_v^\intercal\Sigma_\beta\phi_v \end{aligned} \tag{17}$$

Now, due to Jensen's inequality, we have

$$\mathbb{E}\left\{\hat{A}\right\} = \mathbb{E}\left\{\sqrt{\hat{A}^2}\right\} < \sqrt{\mathbb{E}\left\{\hat{A}^2\right\}} \tag{18}$$

which provides the upper bound on the expectation of $\hat{A}$. The lower bound is obtained by writing $\hat{A}$ on the form

$$\hat{A}(k) = \sqrt{\left(\hat{\alpha}^\intercal\phi_v\right)^2 + \left(\hat{\beta}^\intercal\phi_v\right)^2} = \left\|\hat{k}\right\|_2 \tag{19}$$

with $\hat{k} = [\hat{\alpha}^\intercal\phi_v \quad \hat{\beta}^\intercal\phi_v]$. From Jensen's inequality we have

$$\mathbb{E}\left\{\hat{A}\right\} = \mathbb{E}\left\{\left\|\hat{k}\right\|_2\right\} > \left\|\mathbb{E}\left\{\hat{k}\right\}\right\|_2 = \|k\|_2 = A \tag{20}$$

which concludes the proof. ∎

Corollary 1:

$$\hat{A} = \sqrt{\left(\hat{\alpha}^\intercal \phi_v\right)^2 + \left(\hat{\beta}^\intercal \phi_v\right)^2} \tag{21}$$

is an asymptotically unbiased and consistent estimate of A. *Proof:* Since the least-squares estimate upon which the estimated quantity is based, is unbiased and consistent, the variances in the upper bound in Eq. (14) will shrink as the number of datapoints increases and both the upper and lower bounds will become tight, hence

$$\mathbb{E}\left\{\hat{A}\right\} \to A \quad \text{as} \quad N \to \infty$$

∎

Analogous bounds for the phase function are harder to obtain, but the simple estimator $\hat{\varphi} = \arg \hat{k}$ based on $\hat{k}$ obtained from the least-squares procedure is still asymptotically consistent [8].

Estimates using the least-squares method (3) are, under the assumption of uncorrelated Gaussian residuals of variance σ^2, associated with a posterior parameter covariance $\sigma^2(\mathbf{A}^\intercal\mathbf{A})^{-1}$. This will in a straightforward manner produce confidence intervals for a future prediction of y as a linear combination of the estimated parameters. Obtaining unbiased estimates of the confidence intervals for the functions $A(v,\omega)$ and $\varphi(v,\omega)$ is made difficult by their nonlinear nature. We therefore procede to establish an approximation strategy.

The estimated parameters k are distributed according to a complex-normal distribution $\mathcal{CN}(x+iy,\Gamma,C)$, where Γ and C are obtained through

$$\begin{aligned}
\Gamma &= \Sigma_{xx} + \Sigma_{yy} + i(\Sigma_{yx} - \Sigma_{xy}) \\
C &= \Sigma_{xx} - \Sigma_{yy} + i(\Sigma_{yx} + \Sigma_{xy}) \\
\Sigma &= \begin{bmatrix} \Sigma_{xx} & \Sigma_{xy} \\ \Sigma_{yx} & \Sigma_{yy} \end{bmatrix} = \sigma^2(\tilde{\mathbf{A}}^\intercal\tilde{\mathbf{A}})^{-1}
\end{aligned} \tag{22}$$

For details on the $\mathcal{CN}$-distribution, see, e.g., [9]. A linear combination of squared variables distributed according to a complex normal ($\mathcal{CN}$) distribution, is distributed according to a generalized χ^2 distribution, a special case of the gamma distribution. Expressions for sums of dependent gamma-distributed variables exist, see, e.g., [10], but no expressions for the distribution of linear combinations of norms of Gaussian vectors, e.g., Eq. (10), are known to the authors. In order to establish estimates of confidence bounds on the spectral functions, one is therefore left with high-dimensional integration or Monte-Carlo techniques. Monte-Carlo estimates will be used in the results presented in this paper. The sampling from a $\mathcal{CN}$-distribution is outlined in Proposition 3:

Proposition 3: The vector

$$z = \tilde{x} + i\tilde{y} \in \mathbb{C}^D$$

where

$$\begin{bmatrix} \tilde{x} \\ \tilde{y} \end{bmatrix} = L \begin{bmatrix} x \\ y \end{bmatrix}, \quad x, y \sim \mathcal{N}(0, I) \in \mathbb{R}^D$$

and

$$\Sigma = LL^\intercal$$

is a Cholesky decomposition of the matrix

$$\Sigma = \frac{1}{2}\begin{bmatrix} \Re(\Gamma + C) & \Im(-\Gamma + C) \\ \Im(\Gamma + C) & \Re(\Gamma - C) \end{bmatrix} \in \mathbb{R}^{2D\times 2D}$$

is a sample from the complex normal distribution $\mathcal{CN}(0,\Gamma,C)$. *Proof:* Proof is given in the appendix. ∎

By sampling from the posterior distribution $p(k_\omega|y)$ and propagating the samples through the non-linear functions $A(\omega,v)$ and $\varphi(\omega,v)$, estimates of relevant confidence intervals are easily obtained.

The quality of the estimate thus hinges on the ability of the basis function expansion to appriximate the given functions a and b in Eq. (12). Park [7] provides us with the required result that establishes RBF expansions as a universal function approximator.[4]

F. Comparison to related methods

The act of performing a basis function expansion in $\mathcal{V}$ could be compared to performing windowing along $\mathcal{V}$ with a Gaussian window, with the added constraint $\sum_j \kappa_j(v) = 1$ imposed by the formulation

$$\frac{\kappa_j(v)}{\sum_j \kappa_j(v)} \tag{23}$$

which implies an adaptation of the window to the windows surrounding it.

III. Experimental Results

A. Simulated signals

To asses the qualities of the proposed spectral decomposition method, a test signal y_t is generated as follows

$$\begin{aligned}
y_t &= \sum_{\omega\in\Omega} A(\omega,v)\cos\left(\omega x - \varphi(\omega,v)\right) + e \\
v_t &= \text{linspace}(0,1,N) \\
x &= \text{sort}(\mathcal{U}(0,10)) \\
e &\in \mathcal{N}(0,0.1^2)
\end{aligned} \tag{24}$$

where $\Omega = \{4\pi, 20\pi, 40\pi\}$, the scheduling variable v_t is generated as $N = 500$ equidistantly sampled points between 0 and 1 and x is a sorted vector of uniform random numbers. The sorting is carried out for visualization purposes and for the Fourier based methods to work, this property is not a requirement for the proposed method to work. The functions A and φ are defined as follows

$$\begin{aligned}
A(4\pi,v) &= 2v^2 \\
A(20\pi,v) &= 2/(5v+1) \\
A(40\pi,v) &= 3e^{-10(v-0.5)^2} \\
\varphi(\omega,v) &= 0.5A(\omega,v)
\end{aligned} \tag{25}$$

where the constants are chosen to allow for convenient visualization.

[4] For well behaved functions.

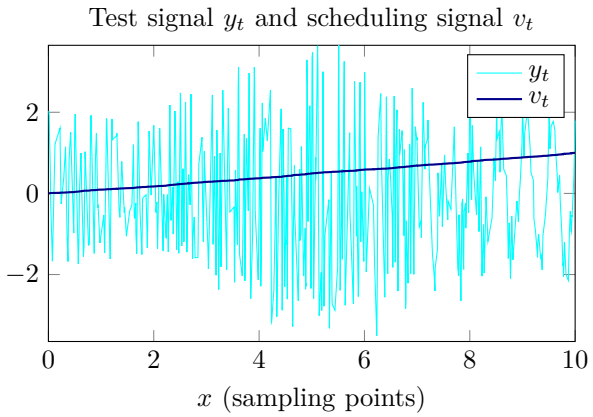

Fig. 2. Test signal with $N = 500$ datapoints. The signal contains three frequencies, where the amplitude and phase are modulated by the functions (25) depicted in Fig. 3.

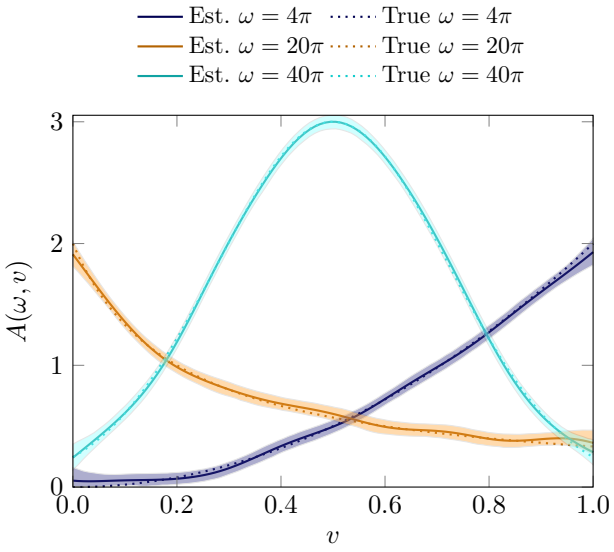

Fig. 3. True and estimated functional dependences with 95% confidence intervals.

The signals y_t and v_t are visualized as functions of the sampling points x in Fig. 2 and the functions A and φ together with the resulting estimates and confidence intervals using $J = 50$ basis functions are shown in Fig. 3. The traditional power spectral density can be calculated from the estimated coefficients as

$$P(\omega) = \left| \sum_{j=1}^{J} k_{\omega,j} \right|^2 \tag{26}$$

and is compared to the periodogram and Welch spectral estimates in Fig. 4. This figure illustrates how the periodogram and Welch methods fail to clearly identify the frequencies present in the signal due to the dependence on the scheduling variable v. The LPV spectral method, however, correctly identifies all three frequencies present.

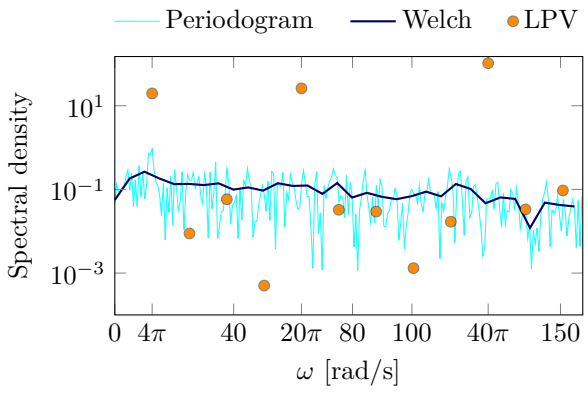

Fig. 4. Estimated spectra, test signal. The periodogram and Welch methods fail to identify the frequencies present in the signal due to the dependence on the scheduling variable v. The LPV spectral method correctly identifies all three frequencies present.

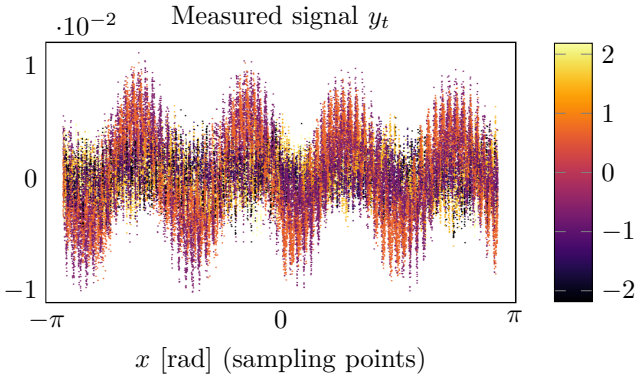

Fig. 5. Measured signal as a function of sampling location, i.e., motor position. The color information indicates the value of the velocity/scheduling variable in each datapoint. Please note this is not a plot of the measured data sequentially in time. This figure indicates that there is a high amplitude periodicity of $4\,\mathrm{rev}^{-1}$ for low velocities, and slightly higher frequencies but lower amplitude signals at $7\,\mathrm{rev}^{-1}$ and $9\,\mathrm{rev}^{-1}$ for higher velocities.

B. Measured signals

The proposed method was used to analyze measurements obtained from an ABB YuMi robot. Due to torque ripple and other disturbances, there is a velocity dependent periodic signal present in the velocity control error, which will serve as the subject of analysis. The analyzed signal is shown in Fig. 5.

The influence of Coulomb friction on the measured signal is mitigated by limiting the support of half of the basis functions to positive velocities and vice versa. A total number of 10 basis functions was used and the model was identified with ridge regression. The regularization parameter was chosen using the L-curve method [11]. The identified spectrum is depicted in Fig. 6, where the dominant frequencies are identified. These frequencies correspond well with a visual inspection of the data. Figure 6 further illustrates the result of applying the periodogram and Welch spectral estimators to data that

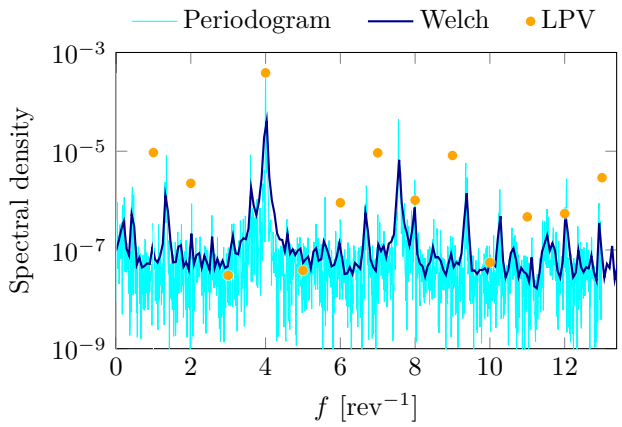

Fig. 6. Estimated spectra, measured signal. The dominant frequencies are identified by the proposed method, while the Fourier based methods correctly identify the main frequency, $4\,\mathrm{rev}^{-1}$, but fail to identify the lower amplitude frequencies at $7\,\mathrm{rev}^{-1}$ and $9\,\mathrm{rev}^{-1}$ visible in the signal in Fig. 5.

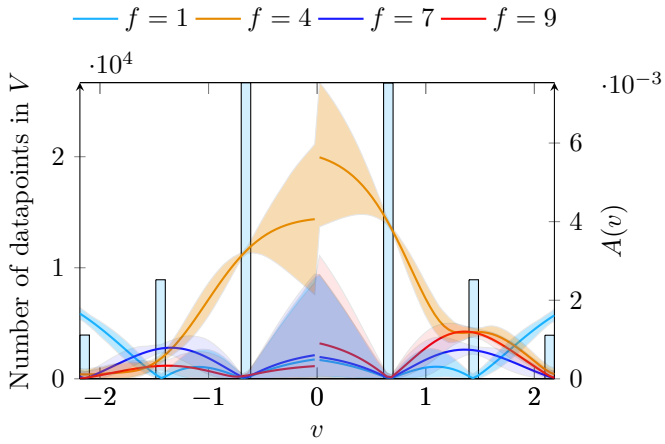

Fig. 7. Estimated functional dependences with 99% confidence intervals. The left axis and histogram illustrates the number of datapoints available at each velocity v. The right axis illustrate the estimated amplitude functions together with their confidence intervals.

has been sorted and interpolated to an equidistant grid. These methods correctly identify the main frequency, $4\,\mathrm{rev}^{-1}$, but fail to identify the lower amplitude frequencies at $7\,\mathrm{rev}^{-1}$ and $9\,\mathrm{rev}^{-1}$ visible in the signal. The amplitude functions for three strongest frequencies are illustrated in Fig. 7, where it is clear that the strongest frequency, $4\,\mathrm{rev}^{-1}$, has most of its power distributed over the lower velocity datapoints, whereas the results indicate a slight contribution of frequencies at $7\,\mathrm{rev}^{-1}$ and $9\,\mathrm{rev}^{-1}$ at higher velocities, corresponding well with a visual inspection of the signal. Figure 7 also displays a histogram of the velocity values of the analyzed data. The confidence intervals are narrow for velocities present in the data, while they become wider outside the represented velocities.

IV. Conclusions

We have developed a spectral estimation method that can decompose the spectrum of a signal along an external dimension, which allows estimation of the amplitude and phase of the sinusoids as functions of the external variable. The method is linear in the parameters which allows for straight-forward calculation of the spectrum through solving a set of linear equations. The method does not impose limitations such as equidistant sampling, does not suffer from leakage and allows for estimation of arbitrary chosen frequencies. The closed-form calculation of the spectrum requires $\mathcal{O}(J^3O^3)$ operations due to the matrix inversion associated with solving the LS-problem, which serve as the main drawback of the method if the number of frequencies to estimate is large (the product JO greater than a few thousands).

An open-source implementation of the method is available at `github.com/baggepinnen/LPVSpectral.jl`.

Appendix

Proof: Proposition 3
Let $v^\mathsf{T} = \begin{bmatrix} x^\mathsf{T} & y^\mathsf{T} \end{bmatrix}$. The mean and variance of $\tilde{v} = Lv$ is given by

$$\mathbb{E}\left\{\tilde{v}\right\} = L\mathbb{E}\left\{v\right\} = 0$$
$$\mathbb{E}\left\{\tilde{v}\tilde{v}^\mathsf{T}\right\} = \mathbb{E}\left\{Lvv^\mathsf{T}L^\mathsf{T}\right\} = LIL^\mathsf{T} = \Sigma$$

The complex vector $z = x + iy \in \mathbb{C}^D$ composed of the elements of v is then $\mathcal{CN}(0, \Gamma, C)$-distributed according to [9, Proposition 1]. ∎

References

[1] D. E. Wells, P. Vanícek, and S. D. Pagiatakis, *Least squares spectral analysis revisited.* Department of Surveying Engineering, University of New Brunswick Fredericton, Canada, 1985.

[2] C. I. Puryear, O. N. Portniaguine, C. M. Cobos, and J. P. Castagna, "Constrained least-squares spectral analysis: Application to seismic data," *Geophysics*, vol. 77, no. 5, pp. V143–V167, 2012.

[3] R. Johansson, *System modeling & identification.* Prentice-Hall, Englewood Cliffs, NJ, 1993.

[4] F. J. Harris, "On the use of windows for harmonic analysis with the discrete fourier transform," *Proceedings of the IEEE*, vol. 66, no. 1, pp. 51–83, 1978.

[5] P. Stoica and R. L. Moses, *Spectral analysis of signals.* Pearson/Prentice Hall Upper Saddle River, NJ, 2005.

[6] K. P. Murphy, *Machine learning: a probabilistic perspective.* MIT press, Cambridge, Massachusetts, 2012.

[7] J. Park and I. W. Sandberg, "Universal approximation using radial-basis-function networks," *Neural computation*, vol. 3, no. 2, pp. 246–257, 1991.

[8] S. M. Kay, *Fundamentals of statistical signal processing, volume I: estimation theory.* Prentice Hall, Englewood Cliffs, NJ, 1993.

[9] B. Picinbono, "Second-order complex random vectors and normal distributions," *IEEE Transactions on Signal Processing*, vol. 44, no. 10, pp. 2637–2640, 1996.

[10] J. F. Paris, "A note on the sum of correlated gamma random variables," *CoRR*, vol. abs/1103.0505, 2011. [Online]. Available: http://arxiv.org/abs/1103.0505

[11] P. C. Hansen, "Regularization tools: A matlab package for analysis and solution of discrete ill-posed problems," *Numerical algorithms*, vol. 6, no. 1, pp. 1–35, 1994.